

# Adaptive Data Rate for Multiple Gateways LoRaWAN Networks

Ulysse COUTAUD  
Semtech Corporation and  
LIG CNRS, Grenoble Alps University  
first.last@univ-grenoble-alpes.fr

Martin HEUSSE  
LIG CNRS, Grenoble INP  
first.last@imag.fr

Bernard TOURANCHEAU  
LIG CNRS, Grenoble Alps University  
first.last@imag.fr

**Abstract**—We propose to optimize the LoRaWAN Adaptive Data Rate algorithm in case an inter-packet error correction scheme is available. We adjust its parameters based on the analysis of the LoRa channel with multiple reception gateways, supported by real-world traffic traces. The resulting protocol provides very high reliability even over low quality channels, with comparable Time on Air and similar downlink usage as the currently deployed mechanism. Simulations corroborate the analysis, both over a synthetic random wireless link and over replayed real-world packet transmission traces.

**Index Terms**—IoT; LoRa; LoRaWAN; LPWAN; QoS; ToA; PER; FEC; ADR; macrodiversity.

## I. INTRODUCTION

Both industry and academia show a growing interest for Low Power Wide Area Networks (LPWAN) and their promise to provide low cost, low power, long range and large scale connectivity for the Internet of Things (IoT). LoRaWAN<sup>®</sup>, a networking protocol specification developed by the open LoRa Alliance<sup>®</sup> on top of Semtech's proprietary modulation LoRa<sup>®</sup>, is one of the leading LPWAN technologies.

The Adaptive Data Rate (ADR) protocol, a key part of LoRaWAN, allows to adjust dynamically the end-device (ED) transmission parameters to adapt to the node transmission conditions and to the network load. If appropriate tuning of the LoRaWAN network has potential to improve performance, the process requires a comprehensive and accurate understanding of the behavior of these networks, in terms of contention and transmission conditions. Moreover, our work stems from the observation that inter-packet FEC (Forward Error Correction) potentially changes the optimal operating point of the network. We base our work on the analysis and modeling of experimental measurements over a public LoRaWAN network with multiple reception gateways. We proceed with the proposition of  $ADR_{opt}$ , an improved version of the LoRaWAN ADR protocol which provides high reliability while preserving the network load. This paper is organized as follow: Section II presents LoRa, LoRaWAN and ADR. Section III describes the experimental traces database construction and how we use it to emulate the use of repetition and FEC.  $ADR_{opt}$  is introduced in Section V with its performance described in Section VI and VII. The state of art is discussed in Section VIII.

## II. LORAWAN PROTOCOL STACK

### A. LoRa Physical Layer

The LoRa modulation [1] uses chirp spread spectrum (CSS) signals to modulate data. A chirp symbol is a linearly increasing frequency ramp mapped cyclically over the radio channel bandwidth ( $BW$ ). The information is encoded by the chirp initial frequency offset. The spreading factor ( $SF$ ) defines the symbol duration, as  $T_{symbol} = \frac{2^{SF}}{BW}$ , and each symbol conveys  $SF$  bits. In the current LoRa implementations,  $SF$  6 to 12 are available. A higher  $SF$  increases the symbol duration, reduces the data rate and makes the modulation more robust.

### B. LoRaWAN

LoRaWAN [2] is an LPWAN protocol stack build on top of the LoRa [1] physical layer. The network topology is cellular-like with several gateways covering the area of interest, often with overlapping coverage zones. The LoRaWAN gateways (GW) relay End Devices (EDs) uplink messages to a central network server (NS). EDs are not associated to a particular GW: the GWs forward all received messages to the NS, and uplink traffic thus benefits from GW diversity. Most of the network complexity is pushed to the NS which handles messages de-duplication, downlink scheduling and routing of uplink data to the application servers. The channel access method is ALOHA: the end-devices initiate their transmissions without any kind of coordination [3]. LoRaWAN typically operates in license-free ISM bands in which the transmission power ( $P_{Tx}$ ) and duty cycle are regulated. In Europe for instance, LoRaWAN networks mostly use sub-bands of the EU868 frequency band in which the limitations are typically  $P_{Tx}$  of 14 dBm and a duty cycle of 1%. LoRaWAN is strongly uplink oriented but each uplink transmission is followed by two short receive windows<sup>1</sup> for the reception of ACKs, downlink traffic or ADR commands (which can all be combined in the same packet). Otherwise, the ED radio remains switched off, which greatly reduces energy consumption. LoRaWAN defines a set of LoRaMAC<sup>®</sup> commands to manage EDs over-the-air. In particular, these downlink commands allow to adapt the uplink transmission parameters such as  $P_{Tx}$ ,  $SF$  and number of frame repetitions ( $Nb_{Trans}$ ). Many limitations of LoRaWAN

<sup>1</sup>The ED might open additional receive windows if it operates in class B (Beacon) or class C (Continuously listening). We focus on class A (All EDs).

in terms of scalability and effective throughput are inherent to ALOHA access [4], [5]. Moreover, ensuring reliable uplink traffic handling by means of ARQ or any kind of feedback is challenging due to very limited downlink traffic capacity [5], [6], even though improvements are possible [7]. Macro-diversity is a central feature of LoRaWAN: all GWs use the same frequency channels and each uplink frame is typically received and forwarded by several GWs. We investigate the benefits of this redundancy and propose to take it into account to optimize the transmission parameters.

### C. Adaptive Data Rate protocol

In the Adaptive Data Rate (ADR) protocol, the NS first estimates the link quality by monitoring the uplink packets metadata. It then adapts periodically the ED transmission parameters via LoRaMAC commands sent in its rare downlink communication opportunities with the ED. If no downlink packet is received for too long, the ED increases its  $P_{Tx}$  and its SF to try to regain connectivity. As the ADR algorithm is not strictly defined by the LoRaWAN specification, implementations may vary. We consider on the ED side (ADR-Node), the Semtech implementation<sup>2</sup>. We consider on the NS side (ADR-NS) the open-source implementation<sup>3</sup> by The Things Networks<sup>4</sup> (TTN):  $ADR_{TTN}$ . This protocol addresses the following three questions by adjusting its internal parameters:

- **How frequently does the ED require a downlink from the NS?**  $ACK\_LIMIT$  and  $ACK\_DELAY$  limit the acceptable number of consecutive uplinks without an ACK command reception. By default,  $ACK\_LIMIT$  and  $ACK\_DELAY$  are respectively 64 and 32 transmissions.
- **How does the NS estimate link quality?**  $ADR_{TTN}$  takes the maximal SNR value witnessed for the last twenty received packets. Even if this maximal value tends to over-evaluate the channel SNR, it is less dependent on the Packet Error Rate (PER) than the average, because the transmissions facing more attenuation are more likely to be missed. Note that this estimation takes into account neither reception by multiple gateways, nor packet repetitions<sup>5</sup>, which both increase the estimated SNR.
- **How conservative should the transmissions parameters selection by the NS be?**  $ADR_{TTN}$  reduces the SF whenever the difference between the current SNR estimation and current SF demodulation floor is more than  $MARGIN$  dB, with a 15 dB default value.  $Nb_{Trans}$  is upper-bounded to 3, increased if  $PER > 0.3$  and decreased if  $PER < 0.05$ .

The algorithms ADR-Node and  $ADR_{TTN}$  are described in more details in the literature [9].

## III. TRANSMISSION TRACES COLLECTION AND ANALYSIS

We built an experimental data-set by recording LoRaWAN transmissions collected by several gateways in an urban area.

<sup>2</sup>Version 1.0.3 [github.com/Lora-net/LoRaMac-node](https://github.com/Lora-net/LoRaMac-node) [8].

<sup>3</sup>[github.com/TheThingsNetwork](https://github.com/TheThingsNetwork).

<sup>4</sup>[thethingsnetwork.org](https://thethingsnetwork.org).

<sup>5</sup>For a given received LoRaWAN packet only the best SNR value is kept.

We then replay the recorded frame series to assess the effect of the adjusting various parameters. In our analysis we distinguish 3 types of losses, at different levels. The Frame Erasure Rate (FER) is the physical loss ratio between the ED and a given GW (i.e. without repetitions). The Packet Error Rate (PER) is the loss ratio between the ED and the NS. PER benefits from multiple gateways reception and frame repetition. The Data Error Rate (DER) is the loss ratio between the ED and the Application Server (AS), thus benefiting from the presence of an application layer inter-packet FEC algorithm.

### A. Setup and experiment

The test-bench consists of one indoor ED<sup>6</sup>, placed on the third floor of a residential building and connected to the TTN open access collecting service through a set of gateways. The device transmits series of LoRaWAN frames and varies the transmission parameters from one frame to the next. The series correspond to all  $(P_{Tx}, SF)$  value pairs, with 48 possible combinations<sup>7</sup>. We used three channels centered on 868.1, 868.3 and 868.5 MHz, with bandwidth  $BW=125$ kHz and using the default LoRaWAN coding rate  $CR=\frac{4}{5}$  for intra-packet FEC. We randomized the transmission parameters in order to avoid shadow correlations and moderate the effect of possibly congested frequency channels. The experiment ran for a whole week and there are on average 4300 frames transmission attempts per series, i.e. one frame every  $\approx 2.4$  minutes with a 15 bytes LoRaWAN payload. Eight TTN GWs showed up within the transmission range of the device. This represents a total of  $48 \times 8 = 384$  independents LoRaWAN series of frames. This set of measures captures the frame erasure patterns over a typical LoRaWAN urban network<sup>8</sup>, and it is publicly available<sup>9</sup>.

### B. Propagation Model Characterization

The experimental data set allows to characterize the channel. For all GWs, we find that the SNR distribution effectively bears some similarity with the exponential distribution of a Rayleigh channel, which appears in red in Fig. 1. This distribution is expected in our setup in which there is no line-of-sight and thus the propagation is likely to be highly multi-path, with no dominant path. Fig. 1 shows the SNR distribution for two of the GWs for SF11 and SF7 for several  $P_{Tx}$ . The histogram does not follow perfectly the exponential distribution: as we reduce  $P_{Tx}$ , the SNR distribution translates towards lower SNR and more and more frames fail to reach the GW sensitivity. The sensitivity of the considered SFs are marked by arrows in Fig. 1. Below this point, most frames are lost, resulting in a progressively more and more censored sample as  $P_{Tx}$  decreases. Notice that there is an artifact at 0 dBm due to bad interpretation of some frames by the monitoring system, which wrongly marks them with a 0 value.

<sup>6</sup>B-L072Z-LRWAN1 LoRa/Sigfox Discovery kit.

<sup>7</sup> $P_{Tx} \in \{0; 2; 4; 6; 8; 10; 12; 14\}$  dBm and  $SF \in [7..12]$ .

<sup>8</sup>Seven GWs deployed in the Grenoble urban area within a 4 km range of the ED and one at 14km with a 1200m higher elevation.

<sup>9</sup>[gricad-gitlab.univ-grenoble-alpes.fr/coutaudu/lora-measurements](https://gricad-gitlab.univ-grenoble-alpes.fr/coutaudu/lora-measurements).

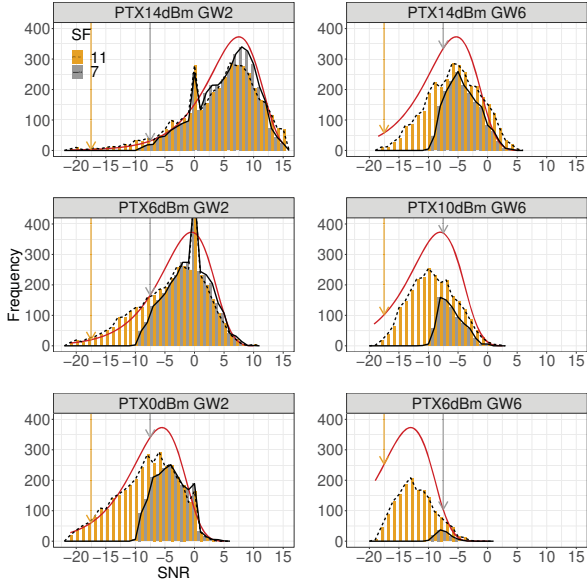


Fig. 1: Distribution of the measured SNR of several LoRaWAN series of frames with SF11 and SF7, compared to an exponential distribution curve in red, for several  $P_{Tx}$ . Arrows mark each SF demodulation floor.

As illustrated by the length of erasure bursts plotted in Fig. 2, the channel is bursty. Moreover, this length increases with the FER. Even over a channel with reasonable FER ( $< 0.3$ ), a significant proportion of the lost frames comes from erasures bursts (length  $\geq 2$ ).

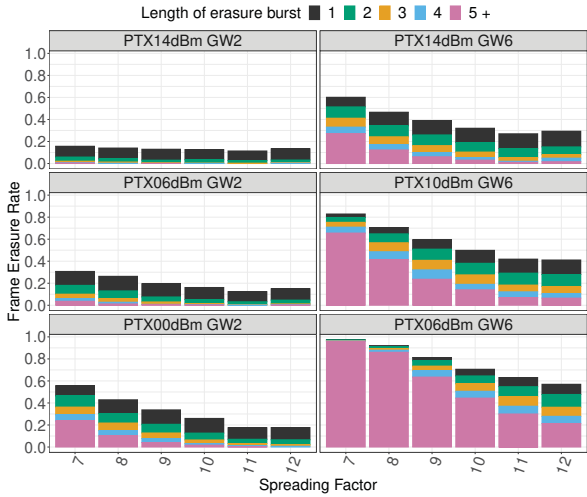


Fig. 2: FER against SF showing the distribution of erasure burst lengths for several LoRaWAN series of frames with two GWs and several  $P_{Tx}$ .

#### IV. FEC CHOICE

With this loss patterns, a scheme based on frame repetition would be successful only for an  $Nb_{Trans}$  significantly larger

than the erasure bursts. So, repetitions quickly become impractical due to high overhead and channel occupation, and other means of improving reliability need to be considered. The solutions based on acknowledgement frames, such as Automatic Repeat reQuest (ARQ), are strongly limited by the asymmetry of LoRaWAN networks where downlink transmission opportunities are scarce [6]. Forward Error Correction (FEC) provides high reliability in LoRaWAN even over a bursty channel [10][11]. Thus, the redundant information to recover from erasures spreads over many frames, introducing time diversity in the communication. In the following we use a FEC scheme based on linear combinations of packets [12]. It does not require additional downlink signaling and it uses more time diversity<sup>10</sup> than the default ADR downlink transmission period<sup>11</sup>.

#### V. IMPROVING ADAPTIVE DATA RATE

Based on the insight gained from our experimental measurements, we propose an NS-side optimized ADR algorithm  $ADR_{opt}$ , detailed in Algo.1 which dynamically adapts the transmission parameters to get the most out of the available radio links. In the following, we consider a constant  $P_{Tx}$ , as  $P_{Tx}$  is reduced from its maximal value only when the signal is very strong and after SF and  $Nb_{Trans}$  have reached their lower values, so the overall performances of ADR in terms of PER and TOA are not affected.

$ADR_{opt}$  extrapolates a presumable PER for each  $[SF; Nb_{Trans}]$  pair from the observation on the channel over the previous transmission period.  $ADR_{opt}$  then chooses the transmission parameters to maintain PER in the target interval. The upper limit of the PER corresponds to the FEC layer implementation to reach full data recovery. Here, with the chosen FEC implementation [12], we need to have  $PER < 0.3$ . The PER ceiling of  $ADR_{opt}$  could be different with another FEC algorithm or without any FEC at all.

The  $ADR_{opt}$  FER estimation function is based on the assumption that the channel is Rayleigh and that the experimental measurements of the SNR follows an exponential distribution with cumulative distribution function  $CDF_{exp}(x) = 1 - e^{-x}$  (and its inverse  $CDF_{exp}^{-1}(x) = -\log(1-x)$ ), multiplied by a factor  $\widehat{SNR}$  corresponding to the estimate of the SNR mean  $\overline{SNR}$ , i.e. the gain shift from unit mean exponential distribution (UMED). For a given GW, we can estimate  $\widehat{SNR}$ , and eventually compute the expected FER in the current channel conditions. As the channel history buffer keeps a limited number of received frames<sup>12</sup>, we have to compute what would be the size of the sample S with its censored part, i.e. the erased frames:

$$size_S = \frac{20}{(1 - PER_{current})} \times Nb_{Trans}$$

We then estimate what would be the maximal value of such a sample following UMED. We approximate the theoretical

<sup>10</sup>In practice, the FEC is computed and spread over 128 frames.

<sup>11</sup>Limited to ACK\_LIMIT+ACK\_DELAY=96 frames.

<sup>12</sup>The TTN NS keeps only the last 20 frames.



**Algorithm 1**  $ADR_{opt}$ -Server algorithm.

---

```

1: ChHistory(20) // Initialization of the list of the last 20 frames
   received.
2:  $PER_{max} = 0.3$ ; // Starts the FEC.
3: while true do
4:   ACK_Req=waitRx();
5:   if (ACK_Req) then
6:     // Compute a prediction of the PER for each configuration.
7:     for all  $GW \in receptionGW(ChHistory)$  do
8:       for  $SF \in \{7; 8; 9; 10; 11; 12\}$  do
9:          $FER = estimateFer(GW, SF, ChHistory)$ 
10:        for  $NbTrans \in \{1; 2; 3\}$  do
11:           $PER_{predic}[SF; NbTrans] = FER^{NbTrans}$ ;
12:        end for
13:      end for
14:    end for
15:     $PER_{target} = PER_{max}$ ;
16:     $PER_{current} = getPER(ChHistory)$ ;
17:    if  $PER_{current} > PER_{max}$  then
18:      // FEC may fail to recover all the lost frames thus
       $PER_{target}$  is reduced to better compensate erasures and achieve
      recovery.
19:       $PER_{target} = \max(0.01, PER_{max} - (PER_{current} - PER_{max}))$ ;
20:    end if
21:    //Choose the best configuration that fits the PER require-
    ment and minimal TOA.
22:     $setValidLowestToAConfig(PER_{predic}, PER_{target})$ 
23:  end if
24: end while

```

---

$SNR_{Max}(S_{UMED})$  by  $SNR_{\approx Max}(S_{UMED})$  that we define as the middle of the interval in which there is 90% chances that this maximum SNR lies, with  $size_S$  trials:

$$SNR_{\approx Max}(S_{UMED}) = \frac{(10 \times \log_{10} (CDF_{exp}^{-1} (0.95^{(1/size_S)})))}{2} + \frac{(10 \times \log_{10} (CDF_{exp}^{-1} (0.05^{(1/size_S)})))}{2}$$

From this we estimate the current average SNR in dB:

$$\widehat{SNR} = ChHistory_{GW}(SNR_{max}) - SNR_{\approx Max}(S_{UMED}).$$

We combine this SNR with the theoretical SNR demodulation floor of LoRa [1] :

$$SNR_{floor < SF} = (-20) + ((12 - SF) * 2.5).$$

Thus the FER is:

$$FER_{< GW_i; SF} = CDF_{exp}\left(10^{\left(\frac{SNR_{floor < SF} - \widehat{SNR}}{10}\right)}\right).$$

For the sake of simplicity, we assume that all repetitions and receptions by different GWs are independent, which leads to:

$$PER_{< NbTrans; SF} \approx \prod_{\forall GW_i} (FER_{< GW_i; SF})^{NbTrans}$$

These formulae compute an accurate approximation of the FER and PER that are necessary to determine the parameters of the FEC necessary to provide good DER. We now have all the elements to optimize the QoS of the LoRa channel using the Rayleigh channel model of Section III-B.

VI.  $ADR_{opt}$  PERFORMANCE SIMULATION

We assume a perfect downlink channel which allows to transmit all the  $ADR_{opt}$  piggybacked commands and parameters into downlink ACKs. The payload overhead produces by inter-packet FEC redundancy can be piggybacked into existing frames and then, the LoRa payload only increases in size from 28 to 50 bytes<sup>13</sup>. As the frame size has little impact on the reception success [13], we do not consider any reception rate penalty for longer frames. The Rayleigh channel describes a series of frames with a fixed SNR mean ( $\overline{SNR}$ ), which corresponds to fixed positions of the node and the gateway. For each frame  $f$ ,  $SNR_f = \overline{SNR} \times X$  where  $X$  is a random variable following the UMED distribution function. Thus, a frame is dropped if  $SNR_f < SNR_{floor < SF}$ . We simulate this for  $\overline{SNR}$  in  $[-30..10]_{dB}$  by steps of 0.5dB with series of 5000 frames repeated 50 times.  $ADR_{opt}$  performance over the simulated Rayleigh channel appears in Fig. 4 in presence of 1, 2, 4 and 8 GWs when the  $\overline{SNR}$  to all GWs are equal. Notice that in a configuration with unequal  $\overline{SNR}$ , GWs with relatively low  $\overline{SNR}$  bring little benefits: the overall performances tends to be the performances of a network with only the best  $\overline{SNR}$  GW, i.e. most of the time the closest one.  $ADR_{opt}$  sharply adapts the transmission parameters and quickly reaches  $DER < 0.01$ . For instance, in Fig. 4  $ADR_{opt}$  provides  $DER < 0.01$  over a single GW network with  $\overline{SNR} \geq -21.5$  dB. This threshold is reduced as the number of GWs increases.  $ADR_{opt}$  provides  $DER < 0.01$  over an 8 GWs network with  $\overline{SNR} \geq -25$  dB to all GWs. The ability to meet the best QoS is conditioned by the most robust available configuration. This sort of "network maximal effort" is in our case SF12 with  $NbTrans = 3$  and FEC. It is also conditioned by the number of GWs in range.

However, as shown in Fig. 4,  $ADR_{opt}$  ToA is higher than  $ADR_{TTN}$  for channels with low  $\overline{SNR}$  ( $-17$  dB and  $-23$  dB for respectively 1 or 8 GWs). This corresponds to the extra energy invested by  $ADR_{opt}$  to achieve a more reliable communication than  $ADR_{TTN}$ . For better  $\overline{SNR}$  values, the transmissions parameters adjustments of  $ADR_{opt}$  are more fine-grained and the same reliability is obtained for lower ToA as shown in Fig. 4.

VII.  $ADR_{opt}$  PERFORMANCE ON REPLAYED TRACES

We ran the experiments over several subsets of our real world transmission records. It appears that the reachable GWs can be classified following their SNR range. Fig. 5 and 6 show the results for these subsets: GWs 3 and 4 that have low SNR (respectively  $\overline{SNR} \approx -8.1$  dB and  $\overline{SNR} \approx -12.1$  dB with  $P_{Tx} = 14$  dBm), GWs 6 and 8 that have medium SNR (respectively  $\overline{SNR} \approx -5.8$  dB and  $\overline{SNR} \approx -6.6$  dB with  $P_{Tx} = 14$  dBm), GWs 2 and 5 that have high SNR (respectively  $\overline{SNR} \approx 4.6$  dB and  $\overline{SNR} \approx -0.4$  dB with  $P_{Tx} = 14$  dBm), and finally the aggregation of GW 2, 3, 4, 5, 6 and 8. Results including GW 1 and 7 are not provided because GW 1 is two meters away from the ED (we simply use it to control the effective transmission of the frames) and reception at GW 7

<sup>13</sup> 13 (LoRaWAN headers) + 15 bytes to 13 + 1 + (15 + 3) × 2 = 37 bytes of payload respectively without and with FEC.

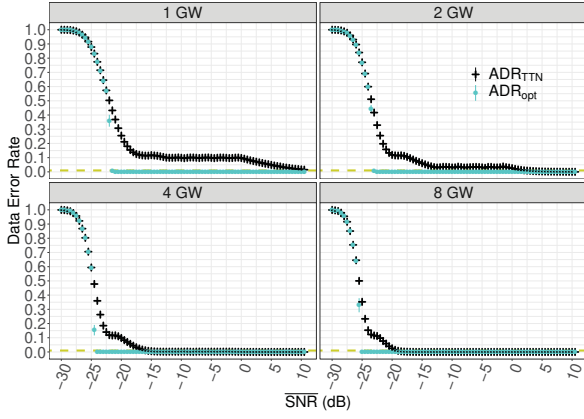


Fig. 3: DER against  $\overline{SNR}$  for the simulated series of frames with a yellow dashed line to mark the 0.01 threshold (99% confidences interval plots).

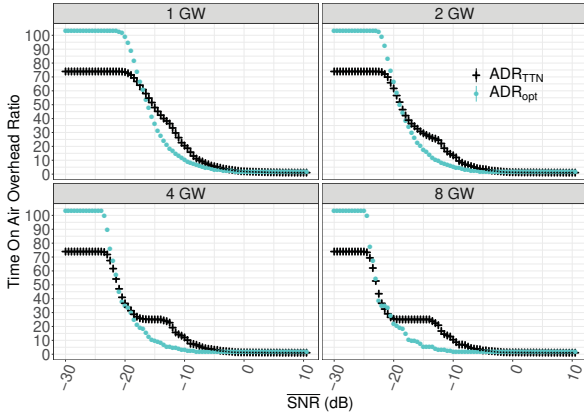


Fig. 4: ToA normalized against no FEC, SF7 and  $Nb_{Trans} = 1$ , against  $\overline{SNR}$  for the simulated series of frames with several GWs (99% confidences interval plots).

is too weak ( $FER \approx 0.9$ ) to bring any benefit alongside the other GWs.

The results derived from our real world transmission traces confirm the simulations of Section VI. For any subset and  $P_{Tx}$  configuration,  $ADR_{opt}$  provides adequate tuning for the transmissions and either  $DER < 0.01$  is achieved or the most robust available configuration is used. Notice that the performances for the subset with GWs 2, 3, 4, 5, 6 and 8 is strongly dominated by the GWs providing the best signal reception, i.e. GWs 2 and 3. As a consequence, its performances is just slightly better than the subset with GWs 2 and 3.

## VIII. STATE OF THE ART

### A. Adaptive Data Rate

Various studies evaluate and improve the ADR's performances. But because the algorithm is not strictly defined by the LoRaWAN specification, various implementations exist and variations of their interpretation appear in the literature.

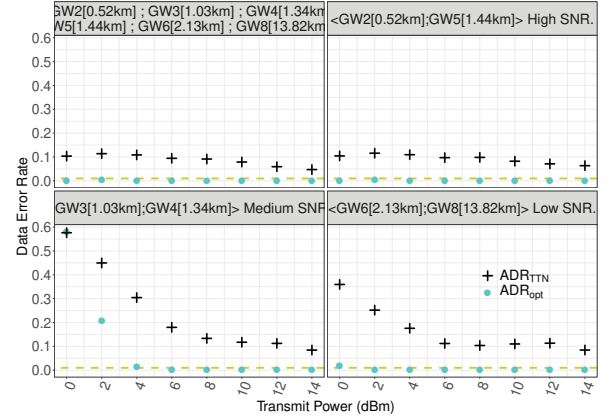


Fig. 5: DER against  $P_{Tx}$  with real world series of frames replays with a yellow dashed line to mark the 0.01 threshold.

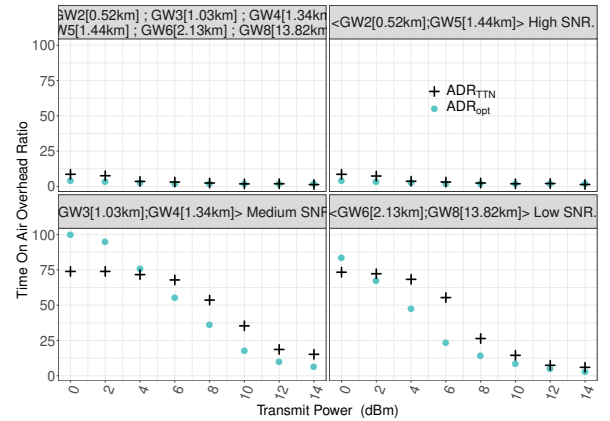


Fig. 6: ToA of several GWs normalized against no FEC, SF7 and  $Nb_{Trans} = 1$ , against  $P_{Tx}$ , for real world series of frames replays.

Some studies [14], [15] suggest that the  $ADR_{TTN}$  tends to overestimate the link quality because of the MAX operator used for the SNR estimation. As a consequence, they suggest to replace it by a MEAN operator. But because the packets with lowest SNR are likely to be more censored, the current path loss' estimation can be biased by both MEAN and MAX. Moreover, the SNR variance has a major influence on the ADR's operation [15]. We think that the SNR distribution pattern and parameters estimation as described in Section V are key for optimized ADR decisions. The ADR can be improved to provides high reliability in a single cell LoRaWAN network by relying on the characterization of the channel as a Rayleigh channel and the use of an application layer FEC algorithm [9]. Our new solution is based on a more accurate estimation of the effective channel, dynamically adapts to the number of GWs in range and fully exploits the macrodiversity, making it more suitable for real world deployment.

The ADR algorithm can be replaced by a load-balancing algorithm to minimize contention on a single cell LoRaWAN network [16]. This approach increases overall throughput

but this may come at the cost of decreasing the network's reliability. An algorithm to select adequate LoRa transmissions parameters to achieve a given reliability between one transmitter and one receiver while reducing energy consumption has been proposed [17]. It starts from the most robust setting and evolves towards a satisfactory setting after the transmission of a few hundreds probes while temporal dynamics is handled by regular restarts. All of this makes it impractically slow compared to our needs.

### B. LoRa/LoRaWAN link characterization

As we consider a context with static EDs and GWs, the Large Scale Fading (LSF) due to the distance and propagation medium path loss exponent between the radios is constant. For the same reason, the Shadow Fading (ShF) from obstructions over the main path is also constant. As a consequence, the variations in the receive signal strength are due to Small Scale Fading (SSF) which corresponds to the gain from multi-path propagation. We neglect the effect of the ambient noise variations, interference, temporal changes of the propagation medium, fast shadowing due to movements around the receiver and transmitter. Thanks to LoRa and LoRaWAN academic and industrial interest, many experimental measurements are reported in the literature.

Three experimental measurements of LoRa link in outdoor environments [18], [11], [19] provide insight into real world link quality variations. They observed a standard deviation of respectively 8 dB, 7.1 dB and between 6.9 dB and 11.2 dB of the channel gain. Notice that among these studies, only one takes into account the censorship of the frames received with low receive power [19].

Another experimental study of the LoRa link characterization over a public LoRaWAN network in a medium sized city [13] shows that the frame's size has relatively small impact on the reception rate and highlight the impact of an initial successful synchronization probability. The behavior of their experimental channel SNR distribution seems to follow a truncated exponential distribution which is expected from a censored Rayleigh channel. The LoRa channel characterization as Rayleigh is also supported by a different study in the same city [9]. LoRa can also be subject to periodic variation of the link quality: an experimental study exposes a periodic 20 dB fading over a 10km LoRa transmissions that may be caused by daily variation of the air's refraction index combined to multi-path propagation [20].

## IX. CONCLUSION

In this paper; we present data gathered from a real world LoRaWAN deployment from which we define a channel model. We use it to derive the expected  $DER$  in presence of multiple GWs and FEC, for any transmission parameters settings. The adaptive data rate  $ADR_{opt}$  algorithm stems from the channel model. It is a significant improvement over the LoRaWAN ADR implemented by TheThingsNetwork, especially in presence of LoRaMAC inter-packet FEC.  $ADR_{opt}$  inherently takes into account macro-diversity and the observed channel variability due to fast fading. The  $ADR_{opt}$

mechanism allows to reach a high level of reliability, with  $DER < 0.01$  in LoRaWAN networks, even for challenging transmission conditions. The  $ADR_{opt}$  proposition is validated both by simulation and by replaying experimental channel transmission traces. Moreover,  $ADR_{opt}$  does not necessitate any additional downlink transmissions compared to the legacy LoRaWAN ADR. The  $ADR_{opt}$  Time on Air is bounded by the maximal effort configuration, warrants scalability and makes it a realistic option for current and future deployments.

Our future work will extend  $ADR_{opt}$  to take into account contention and better balance the load between the different SFs, frequency channels and FEC parameters.

## REFERENCES

- [1] Semtech Corporation, "LoRa® Modulation Basics," Tech. Rep. AN1200.22, 2015.
- [2] N.Sornin and A.Yegin, "LoRaWAN® 1.0.3," LoRa Alliance, Tech. Rep., 2018.
- [3] N. Abramson, "Development of the alohanet," *IEEE Transactions on Information Theory*, vol. 31, no. 2, pp. 119–123, 1985.
- [4] O. Georgiou and U. Raza, "Low power wide area network analysis: Can LoRa scale?" *IEEE Wireless Communications Letters*, vol. 6, no. 2, pp. 162–165, 2017.
- [5] F. Adelantado, X. Vilajosana, P. Tuset-Peiro, B. Martinez, and J. Melia, "Understanding the limits of LoRaWAN," *IEEE Communications*, vol. 55, no. 9, 2017.
- [6] A.-I. Pop, U. Raza, P. Kulkarni, and M. Sooriyabandara, "Does bi-directional traffic do more harm than good in LoRaWAN based LPWA networks?" in *Global Communications (GLOBECOM)*. IEEE, 2017.
- [7] V. Di Vincenzo, M. Heusse, and B. Touranacheau, "Improving downlink scalability in LoRaWAN," in *International Conference on Communications (ICC)*. IEEE, 2019.
- [8] LoRa Alliance, "Lorawan® 1.0.3 revision A regional parameters," Tech. Rep., 2018.
- [9] U. Coutaud, M. Heusse, and B. Touranacheau, "High reliability in lorawan," in *Symposium on Personal, Indoor and Mobile Radio Communications (PIMRC)*. IEEE, 2020.
- [10] U. Coutaud and B. Touranacheau, "Channel coding for better QoS in LoRa networks," in *Wireless and Mobile Computing, Networking and Communications (WiMob)*. IEEE, 2018.
- [11] P. J. Marcellis, V. Rao, and R. V. Prasad, "DaRe: Data recovery through application layer coding for LoRaWAN," in *Internet-of-Things Design and Implementation*. ACM, 2017.
- [12] U. Coutaud, M. Heusse, and B. Touranacheau, "Fragmentation and forward error correction for LoRaWAN small MTU networks," in *Embedded Wireless Systems and Networks (EWSN)*. ACM, 2020, pp. 289–294.
- [13] T. Attia, M. Heusse, B. Touranacheau, and A. Duda, "Experimental Characterization of LoRaWAN Link Quality," in *Global Communications Conference (GLOBECOM)*. IEEE, 2019.
- [14] V. Hauser and T. Hégr, "Proposal of adaptive data rate algorithm for LoRaWAN-based infrastructure," in *Future Internet of Things and Cloud (FiCloud)*. IEEE, 2017.
- [15] M. Slabicki, G. Premsankar, and M. Di Francesco, "Adaptive configuration of LoRa networks for dense IoT deployments," in *Network Operations and Management Symposium (NOMS)*. IEEE/IFIP, 2018.
- [16] S. Kim and Y. Yoo, "Contention-aware adaptive data rate for throughput optimization in LoRa wan," *Sensors*, vol. 18, no. 6, 2018.
- [17] M. Bor and U. Roedig, "Lora transmission parameter selection," in *Distributed Computing in Sensor Systems (DCOSS)*. IEEE, 2017.
- [18] J. Petajajarvi, K. Mikhaylov, A. Roivainen, T. Hanninen, and M. Pet-tissalo, "On the coverage of LPWANs: range evaluation and channel attenuation model for LoRa technology," in *ITS Telecommunications (ITST)*. IEEE, 2015.
- [19] G. Callebaut and L. Van der Perre, "Characterization of LoRa point-to-point path-loss: Measurement campaigns and modeling considering censored data," *IEEE Internet of Things Journal*, 2019.
- [20] T. Ameloot, P. Van Torre, and H. Rogier, "Periodic LoRa signal fluctuations in urban and suburban environments," in *European Conference on Antennas and Propagation (EuCAP)*. IEEE, 2019.